View metadata, citation and similar papers at core.ac.uk

brought to you by CORE

provided by Queensland University of Technology ePrints Archive

COVER SHEET

This is the author version of article published as:

Gramotnev, Dmitri K. (2005) Adiabatic nano-focusing of plasmons by sharp metallic grooves: Geometrical optics approach . *Journal of Applied Physics* 98:104302.

Copyright 2005 American Institute of Physics

Accessed from http://eprints.qut.edu.au

Adiabatic nano-focusing of plasmons by sharp metallic grooves: geometrical optics approach.

D. K. Gramotnev

Applied Optics Program, School of Physical and Chemical Sciences, Queensland University of Technology, GPO Box 2434, Brisbane, QLD 4001, Australia.

(Received

ABSTRACT

In this paper, we demonstrate the possibility of efficient adiabatic nano-focusing of gap plasmons by sharp metallic V-grooves or dielectric wedges covered with metal. Geometrical optics approach and the approximation of continuous electrodynamics are used for the analysis. In particular, it is demonstrated that both the phase and group velocities of an incident symmetric (with respect to the magnetic field) plasmon tend to zero at the tip of the groove, and the plasmon adiabatically slows down, eventually dissipating in the metal. The amplitude of the plasmon strongly increases near the tip of the groove. However, unlike nano-

focusing by a sharp metal conical tip, even in the absence of dissipation, the amplitude of the plasmon near the tip of a V-groove remains finite. The dependence of the maximal local field enhancement on structural parameters, dissipation in the metal, angle of incidence, etc. is analyzed. It is also shown that a symmetric gap plasmon can effectively be guided by the groove, forming a channel plasmon-polariton – a special plasmon mode propagating along the tip of a metallic V-groove. A new existence condition for these strongly localized plasmon-polaritons is derived and discussed.

PACS codes: 78.67.–n; 68.37.Uv; 73.20.Mf

1. INTRODUCTION

One of the major directions of research in modern photonics and nano-optics is related to the theoretical, numerical, and experimental investigation of strongly localized plasmons in metallic nano-structures. This is because these waves and structures offer unique opportunities for design of new plasmonic devices and waveguides for integrated optics with sub-wavelength localization [1-21], high-resolution near field optical microscopy [2,22-30], and strong increase of local field resulting in such non-linear effects as, for example, giant surface enhanced Raman scattering [30-34], etc.

A number of different metallic nano-structures have recently been considered for the development of efficient sub-wavelength plasmonic waveguides. These include metallic nano-rods [6,7] and nano-strips [8-11], nano-chain waveguides made of periodically spaced metallic nano-particles [3-5], waveguides in the form of a metallic trapezium nano-wedge [12,13], and waveguides with gap plasmons [14-16].

Recently, a new type of plasmonic sub-wavelength waveguide with a number of superior features has been suggested and described [17-19]. This waveguide is formed by a V-

groove on a metal surface, and a strongly localized channel plasmon-polariton (CPP) propagates along this groove, being localized near its tip [17-20]. The localization of CPP near the tip depends on the groove angle, decreasing which results in a rapid increase of the CPP localization near the tip. Typical values of the groove angle that are required for strong sub-wavelength localization are usually below ~ 30^o – 40^o [17-19]. The main advantages of the considered groove plasmonic waveguides include strong sub-wavelength localization [17-19], relatively weak dissipation and larger propagation distances [17,18], broad-band transmission [17-19], possibility of nearly 100% transmission through sharp bends [19], single-mode operation achieved simply be reducing depth of the groove, so that higher modes are not guided by the structure [18], a possibility of design of effective filters and Fabry-Perot resonators [21], etc.

One of the major problems of nano-optical design is related to difficulties with efficient coupling of light into metallic nano-structures and waveguides. This is because an incident laser beam cannot be focused by means of the conventional optics into a region that is less than $\lambda/(2n)$ (the diffraction limit of light), where λ is the wavelength in vacuum and n is the refraction index of the medium. Therefore, creating nano-scale optical devices and interconnectors does not make much sense without being able to effectively communicate with each of these devices/waveguides without interference with other integrated elements. This, however, is difficult to achieve by means of the conventional optics due to its insufficient resolution.

One of the possible solutions of this problem is associated with adiabatic nano-focusing of light by metallic nano-structures [22-27]. Nano-focusing is concentration/focusing of light into a region with dimensions that are significantly smaller than those allowed by the diffraction limit of light. It also results in strong enhancement of local electromagnetic fields in the region of focusing, for example, near the tip of a tapered optical fiber covered with metal [24-26], at the tip of a metallic nano-rod [27,30], or near the tip of a triangular probe of

a near-field optical scanning microscope [28,29]. For example, it has been demonstrated that in the approximation of the continuous electrodynamics and in the absence of dissipation, the amplitude and localization of a plasmon propagating along a tapered metallic nano-rod tend to infinity as the plasmon approaches the tip [27]. This type of nano-focusing is to some extent analogous to using a spherical lens in the conventional optics, but with much stronger field localization at the focus (i.e., at tip of the tapered rod). Both phase and group velocities of the plasmon were shown to decrease to zero at the tip of a sufficiently sharp conical metal tip [27], the plasmon asymptotically stops and eventually dissipates in the metal.

Similar situation can be expected to occur in the case of gap plasmons propagating in a metallic gap with slowly varying width (sharp V-shaped groove). Such two-dimensional nano-focusing will be analogous to a cylindrical lens for bulk waves, but with a much stronger field localization in the focal line (at tip of the groove). Experimentally, such focusing and strong enhancement of the local field have been observed in [28,29]. However, the current absence of a consistent theory of adiabatic plasmon nano-focusing by wedge-like structures results in a lack of physical understanding of the phenomena associated with near-field optical microscopy [2,27-29] and sub-wavelength localization in metallic nano-structures. The current unanswered questions include absence of understanding of physical limitations of the two-dimensional nano-focusing, optimization of the focusing structures, the effect of dissipation in the metal on the local field enhancement, etc.

Therefore, the main aim of this paper is to investigate theoretically adiabatic nano-focusing of plasmons by a sharp V-groove in a metal, filled with dielectric (dielectric wedge with slowly varying thickness covered by metal). Geometrical optics approach (GOA) will be used for the analysis of symmetric (with respect to magnetic field) gap plasmons incident onto the tip of a sharp groove (gap with slowly varying width). Strong enhancement of the amplitude of an incident symmetric gap plasmon, and adiabatic decrease of its phase and group velocities to zero will be shown to occur near the tip of the groove with and without dissipation

in the metal. We will also show that a CPP mode in a sufficiently sharp groove can be represented by a gap plasmon successively reflecting from the tip of the groove and a turning point (simple caustic). As a result, a new existence condition for CPP modes, i.e. a lower critical angle of the groove, below which CPP modes are infinitely localized (i.e., do not exist), will be determined.

2. GEOMETRICAL OPTICS APPROXIMATION FOR GAP PLASMONS

The analyzed structure is presented in Fig. 1a. A deep V-groove with a small angle β (the conditions restricting β are presented below) is formed in a metal with the complex permittivity $\varepsilon_2 = e_1 + ie_2$ ($e_1 < 0$, $e_2 > 0$). The coordinate axes are as indicated in the figure. The depth of the groove along the y-axis is assumed to be sufficiently large, so that two plasmons propagating on the opposite sides of the groove at the top of the groove can be regarded as uncoupled (i.e., the maximal width of the groove should noticeably exceed the penetration depth of the surface plasmons into the dielectric material filling the groove). For mathematical simplicity, we will assume that the depth of the groove is infinite. The dielectric permittivity ε_1 of the material inside the groove is real and positive, and $|e_1| > \varepsilon_1$ (existence condition for surface and gap plasmons [35]).

Consider two surface plasmons of the same frequency on the opposite sides of the groove, both propagating towards the tip of the groove at the same angle of incidence with respect to the y-axis. At a large distance from the tip of the groove, where these plasmons can be regarded uncoupled, this angle of incidence is θ_0 (Fig. 1b). As the two plasmons travel towards the tip of the groove, the width of the groove becomes smaller, and eventually the plasmons become coupled across the gap (groove), forming a gap plasmon. If the magnetic fields in the two incident surface plasmons are in phase with each other, and have the same amplitudes, then the resultant gap plasmon will be a symmetric gap plasmon. If the magnetic fields in the incident plasmons are in antiphase, and have the same amplitudes, then the resul-

tant gap plasmon will be an antisymmetric gap plasmon. In this paper, we will mainly concentrate on propagation of symmetric gap plasmons (with symmetric distribution of the magnetic field across the gap). These plasmons do not have a cut-off gap width and can exist in arbitrarily narrow gaps, i.e., arbitrarily close to the tip of the groove.

As the symmetric gap plasmon propagates towards the tip of the groove, it will experience changing width of the groove (gap). This means that the effective dielectric permittivity of the structure $\varepsilon_{eff} = (q/k_0)^2$ also changes. Here, q is the wave number of the symmetric gap plasmon (depending on gap width h), and $k_0 = \omega/c$, where ω is the angular frequency of the wave, and c is the speed of light in vacuum. Propagation of the gap plasmon can be considered in the geometrical optics approximation (GOA) (or, using the terminology of quantum mechanics, in the WKB approximation), if variations of the wave vector of the plasmon are small within distances of the order of one wavelength in the structure [27,36]:

$$|d(Q_{1y}^{-1})/dy| << 1, \qquad (1)$$

where Q_{1y} is the y-component of the real part of the wave vector **q** of the gap plasmon in the groove (Fig. 1b). If condition (1) is satisfied for all values of y, then the symmetric plasmon can be approximated by a plane wave at any point along the direction of its propagation (along a plasmon ray – Fig. 1b), and the groove can be regarded as a gap with slowly varying width. The distribution of the field, dispersion and dissipation of the gap plasmon will then be approximately the same as for the plasmon in a uniform gap of the width that is equal to the local width of the V-groove at the considered point on the plasmon ray (i.e., at the considered distance from the tip of the groove – Fig. 1).

The wave number of a symmetric gap plasmon is given by the dispersion relation obtained from the Maxwell equations and the conventional boundary conditions at the gap boundaries:

$$\tanh\left(\frac{\alpha_1 h}{2}\right) = -\frac{\alpha_2 \varepsilon_1}{\alpha_1 \varepsilon_2}, \qquad (2)$$

where

$$\alpha_1 = \sqrt{q^2 - k_0^2 \varepsilon_1}, \qquad \alpha_2 = \sqrt{q^2 - k_0^2 \varepsilon_2}, \qquad (3)$$

h is the local width of the V-groove (gap):

$$h = 2y \tan(\beta/2), \qquad (4)$$

Let us now assume that dissipation is weak, i.e. $e_2 << |e_1|$. The opposite case is not interesting, since if dissipation is strong, the plasmon will not be able to propagate noticeable distances in the structure. If dissipation is weak, then $Q_2 << Q_1$, where Q_1 and Q_2 are the real and imaginary parts of the complex wave number $q = Q_1 + iQ_2$. In this case, if the gap width is small: $h \to 0$ (e.g., at the tip of the groove) and

$$h\mathrm{Re}(\alpha_1) << 1, \qquad (5)$$

then Eq. (2) can be simplified as:

$$Q_1 \approx -2\varepsilon_1/(e_1 h). \qquad (6)$$

Note that Eqs. (5) and (6) are consistent with each other only if $\varepsilon_1/|e_1| << 1$, which is usually the case for good metals. Eq. (6) suggests that decreasing h to zero results in increasing wave number of the gap plasmon to infinity, which is equivalent to decreasing its wave length to zero. As a result, the phase velocity of the plasmon $v_{ph} = \omega/Q_1 \to 0$, when $h \to 0$ (or $y \to 0$ near the tip of the groove – Fig. 1). Similarly, in this approximation, the group velocity of the plasmons $v_g = \partial\omega/\partial Q_1 \approx h e_1^2 (2\varepsilon_1 de_1/d\omega)^{-1} \to 0$ as $h \to 0$ (i.e., near the tip of the groove).

The same result can be obtained from the direct numerical solution of Eq. (2). In this case, condition (5) is not necessary. The numerical dependencies of the wave number Q_1 of a

symmetric plasmon on gap width h are presented in Fig. 2a for different dielectric permittivities of the metal and dielectric filling the groove. The presented values of e_1 correspond to silver at the indicated wavelengths – see the figure caption.

It can be seen that decreasing h to zero results in a rapid in crease of the wave number of the gap plasmon. This increase is faster for smaller magnitudes of the metal permittivity and larger amplitude of the permittivity of the dielectric filling the groove. It can be said that for every gap thickness h, increasing the ratio $\varepsilon_1/|e_1|$ results in a monotonous increase of the wave number of the symmetric gap plasmon.

Eq. (6) and Fig. 2a suggest that in GOA, gap plasmons asymptotically stop at the tip of the groove, similarly to strongly localized one-dimensional plasmons stopping at the tip of a sufficiently sharp metallic cone [27]. This will occur for all angles of incidence $\theta_0 < \pi/2$ (Fig. 1b). As the plasmon propagates towards the tip of the groove, the y-component Q_{1y} of the real part of its wave vector $\mathbf{Q}_1$ will increase to infinity. Therefore, irrespectively of the initial incidence angle θ_0 (as long as $\theta_0 < \pi/2$), the wave vector of the plasmon near the tip is perpendicular to the x-axis, which makes the plasmon ray turn perpendicular to the tip of the groove Fig. 1b. Note however, that all these conclusions are correct only if the applicability condition (1) for GOA is satisfied for all values of y. In this case, no reflection occurs from the tip of the groove – the plasmon propagates towards the tip, adiabatically slows down, and eventually dissipates in the metal.

Fig. 2b presents the y-dependencies of the left-hand side of condition (1) for the considered silver-dielectric structure with the groove angle $\beta = 2^o$. For all values of y (distance from the tip of the groove – Fig. 1), at which the graphs in Fig. 2b are significantly below 1, GOA is applicable. It can be said that for the structures corresponding to curves 3 – 5 GOA is applicable for all distances from the tip of the groove, while for the structures corresponding to curves 1 and 2 GOA is applicable only for $y \gtrsim 0.1$ μm. It can be seen that increasing per-

mittivity of the dielectric in the gap results in improving applicability of GOA (compare curves 2 and 4, and curves 3 and 5). Increasing magnitude of the real part of the metal permittivity results in worsening applicability of GOA (compare curves 1, 2 and 5). This is because the wave vector of the gap (and surface) plasmon increases, and the wavelength decreases, if $\varepsilon_1 \to |e_1|$. As a result, variations of the gap width within one wavelength become smaller, which ensures better applicability of GOA. Decreasing angle of the groove also results in improving applicability of GOA (compare curves 2 and 4).

At large distances from the tip, GOA is always applicable, since in this case the two surface plasmons forming the symmetric gap plasmon become uncoupled. Therefore, slow or rapid variations of the gap width hardly affects their dispersion (as long as the width of the gap is noticeably larger than the penetration depth of the surface plasmons into the dielectric).

It is interesting that near the tip, the applicability condition for GOA (Eq. (1)) can be significantly simplified, which results in important conclusions about the behavior of plasmons in the considered structures. Using Eqs. (4) and (6), taking into account that near the tip (at $h \to 0$) $Q_{1y} \approx Q_1$, and considering small groove angles $\beta << 1$, condition (1) can be reduced as:

$$\left|\frac{d(Q_{1y}^{-1})}{dy}\right| \approx -\frac{\beta e_1}{2\varepsilon_1} << 1, \tag{7}$$

or

$$\beta << \beta_{c2} = -2\varepsilon_1/e_1, \tag{8}$$

where β_{c2} is the critical angle of the groove, such that GOA is applicable only for angles that are significantly smaller than β_{c2} (the reason for using index 2 will be clear in section 4).

For example, for the silver-vacuum structure and the vacuum wavelength λ_{vac} = 0.6328 μm (He-Ne laser) we have: $e_1 = -16.22$ [37,38], and $\beta_{c2} \approx 7^o$. This is the reason why curve 3 in Fig. 2b, corresponding to the groove angle $\beta = 2^o$ lies significantly below 1, and thus the applicability condition for GOA is approximately satisfied.

It is interesting that the left side of inequality (7) does not depend on gap width h. This is the reason why all the graphs in Fig. 2b reach plateaus at small values of y. The dependencies in Fig. 2b tend to $-\beta e_1/(2\varepsilon_1)$ as $y \to 0$.

If condition (8) is not satisfied (i.e., $\beta \gtrsim \beta_{c2}$), then GOA is not applicable near the tip of the groove, and the incident plasmon may experience noticeable reflection from the tip. Physically, these reflections will take at every point on the ray where the applicability condition for GOA is not satisfied. Decreasing real part of the metal permittivity e_1 and increasing permittivity ε_1 of the dielectric medium in the groove result in increasing critical angle β_{c2}, and the applicability condition for GOA becomes less restrictive (curves 1, 2 and 5 in Fig. 2b).

3. PLASMON RAYS

A plasmon ray, i.e. a curve parallel to the direction of the wave vector of the plasmon at any point on this curve (or trajectory along which the plasmon propagates in the structure), is determined by the angle θ between this ray and the y-axis (Fig. 1b). This angle at a arbitrary value of y can be determined from the Snell law which suggests that the x-component of the wave vector of the plasmon must be independent of y (since the structure is uniform along the x-axis). Therefore,

$$Q_{01}\sin\theta_0 = Q_1\sin\theta, \tag{9}$$

where Q_{01} is the real part of the wave number $q_0 = Q_{01} + iQ_{02}$ of the gap plasmon at $y \to +\infty$. Note that since at $y \to +\infty$ the two plasmons on the groove sides are uncoupled, q_0 must be equal to the wave number of a plasmon on an isolated interface between the media with the permittivities ε_1 and ε_2 [35]:

$$q_0 = \frac{\omega}{c}\sqrt{\frac{\varepsilon_1\varepsilon_2}{\varepsilon_1+\varepsilon_2}}\,. \tag{10}$$

If dissipation is weak, i.e., $Q_2 << Q_1$, then a plasmon ray can be determined by the following algorithm. The real part of the plasmon wave number Q_1 is approximately determined by Eq. (2) with ε_2, α_1, and α_2 being replaced by e_1 and α_{01}, and α_{02}, respectively:

$$\tanh\left(\frac{\alpha_{10}h}{2}\right) = -\frac{\alpha_{20}\varepsilon_1}{\alpha_{10}e_1}, \tag{11}$$

where

$$\alpha_{10} = \sqrt{Q_1^2 - k_0^2\varepsilon_1}\,, \qquad \alpha_{20} = \sqrt{Q_1^2 - k_0^2 e_1}\,. \tag{12}$$

Eq. (11) is solved numerically to determine Q_1 as a function of gap width h. Then, choose an incidence angle $0 \le \theta_0 < \pi/2$, at which the gap plasmon propagates with respect to the y-axis at sufficiently large distances from the tip of the groove, where the two surface plasmons forming the incident symmetric gap plasmon are approximately uncoupled (Fig. 1b). Then the angle θ between the plasmon ray and the y-axis at any point on the ray is given by Eq. (9). Therefore, if we know the position of some point with the coordinates (x,y) on the ray, then the position of the next point with the coordinated (x + dx, y + dy) on the same ray is determined by the angle θ at the point (x,y) and the value of dy. Thus, the plasmon ray can be determined if we know the position of some the initial point through which the plasmon ray

propagates. Suppose that this point is chosen on the y-axis. Then the typical plasmon rays for different incidence angles θ_0 and different groove angles are presented in Fig. 3.

All the curves in Fig. 3 are orthogonal to the x-axis at y = 0. As indicated above, this is because at the tip of the groove, the y-component of the wave vector of the gap plasmons turns to infinity.

It is interesting to note that the plasmons rays are determined only by the Snell law. Applicability conditions for GOA should not necessary be satisfied in order to determine the curves that are parallel to the direction of the wave vector of the plasmons. Therefore, the proposed procedure and the typical plasmon rays do not depend on whether GOA is applicable or not. At the same time, if GOA is not applicable, plasmons should experience reflection in the groove, and there should be rays corresponding to the reflected plasmons.

4. NANO-FOCUSING OF GAP PLASMONS

If a gap plasmon propagates along a ray determined in Section 3, then in the absence of dissipation the y-component of the energy flux in this plasmon must be constant along the ray. Indeed, consider a plane plasmon wave incident onto the tip of the groove at an angle θ_0, and consider a box that has sufficiently large dimensions along the z-axis, so that the field of the gap plasmon is significant only for values of z inside the box (Fig. 4).

Since the structure is uniform along the x-axis (along the tip of the groove), the energy inflow into the box through its left side is exactly cancelled by the energy outflow through the right side (Fig. 4). Therefore, the energy conservation in the box suggests that the y-component of the energy flux $\mathbf{S}_1$ (per unit length of the x-axis) in the gap plasmon at the top side of the box must be equal to the y-component of the energy flux $\mathbf{S}_2$ in the gap plasmon at the bottom side of the box. If, for example, the top side of the box is far away from the tip, so

that the two surface plasmons forming the gap plasmon are uncoupled, then energy conservation in the box gives

$$S_0\cos\theta_0 = S\cos\theta, \tag{13}$$

where S_0 is the energy flux in the gap plasmon (i.e. two uncoupled surface plasmons) at large distance from the tip of the groove, and S and θ are the energy flux and angle of propagation of the plasmon at an arbitrary point on the plasmon ray (for simplicity, we have omitted here the index 2 for the energy flux at the bottom side of the box Fig. 4). Note again that Eq. (13) is valid only in the assumption of zero dissipation in the metal.

The energy flux S in the gap plasmon at an arbitrary gap width h is given by the Poynting vector averaged over the period of the wave $\omega/2\pi$ and integrated over the z-coordinate from $-\infty$ to $+\infty$:

$$S = \frac{c^2 Q_1}{16\pi\omega}\left|H_{20}\right|^2\left[\frac{2}{\varepsilon_2\alpha_{20}} + \frac{\sinh(\alpha_{10}h)}{\varepsilon_1\alpha_1\cosh^2(\alpha_{10}h/2)} + \frac{h}{\varepsilon_1\cosh^2(\alpha_{10}h/2)}\right], \tag{14}$$

where H_{20} is the amplitude of the magnetic field at either of the metal interfaces.

Thus, in order to obtain the amplitude of the incident plasmon as a function of distance from the tip of the groove in the absence of dissipation, we use the following procedure. Determine (numerically) Q_1 from Eq. (11) for different values of h (Fig. 2a), which automatically gives the dependence of Q_1 on y – see Eq. (4). Then we use Eq. (9) to determine the angle θ between the wave vector of the gap plasmon and the y-axis as a function of y, calculate S(y) from Eq. (14), and use Eq. (13) to determine the amplitude of the plasmon $H_{20}(y)$, assuming that the amplitude of the incident plasmon at infinity $H_{200} = 1$ (recall that we consider the structure without dissipation).

The corresponding y-dependencies of the plasmon amplitude $H_{20}(y)$ are presented in Figs. 5a,b for zero dissipation in the metal ($Q_2 = 0$). In particular, it can be seen that as the plasmon propagates towards the tip of the groove, a significant increase in its amplitude occurs, resulting in a nano-focusing effect in the considered groove structure. However, it is important to understand that contrary to nano-focusing by means of a sharp conical tip [27], the enhancement of the local field in a sharp groove is finite even in the absence of dissipation, despite the decrease to zero of the wavelength and both phase and group velocities of the plasmon near the tip (similar to [27]). As can be seen from Figs. 5a,b, the maximal enhancement of the local field near the tip in real situations is limited by a factor of ~ 10 or less, and the y-dependences of the plasmon amplitude tend to plateaus at small values of y (or h). The same result can also be seen directly from Eq. (14). Indeed, if $h \to 0$ and condition (5) is satisfied, then $\alpha_{10} \approx \alpha_{20} \approx Q_1$, Q_1 is given by Eq. (6), and Eq. (14) can be reduced as

$$S \approx -\frac{c^2}{8\pi\omega\varepsilon_2}\left|H_{20}\right|^2, \tag{15}$$

which is independent of h (or y). Therefore, at sufficiently small values of h (or y) the energy flux in a symmetric plasmon does not vary with variations of gap width, despite the fact that the wavelength of the plasmon (and its phase and group velocities) tend to zero when $h \to 0$. The Poynting vector in the plasmon increases with increasing Q_1, but this is cancelled by increasing localization of the plasmon (due to decreasing its wavelength), resulting is the total energy flux S in the plasmon being independent of h (at sufficiently small h).

In practice, sharp grooves with an ideal triangular shape are not achievable due to atomic structure of matter. In addition, the discussed approach is based upon the approximation of the continuous electrodynamics, which is applicable only down to dimensions of the tip of ~ 1 nm [39,40]. Below these dimensions, spatial dispersion of the dielectric permittivity has to be taken into account [27,39,40]. However, it is important that the maximal achievable

enhancement of the local field in the considered structures is achieved at the distances from the tip of ~ 30 nm (Fig. 5), which corresponds to the size of the tip of ~ 1 nm. Therefore, the maximally achieved enhancement of the local field can be considered in the assumed approximation of continuous electrodynamics for most of practically reasonable structures.

Increasing dielectric permittivity of the metal results in increasing amplitude of the plasmon near the tip of the groove (compare curves 1 and 4 in Fig. 5a). On the other hand, increasing permittivity of the dielectric filling the gap (groove) results in decrease of the field enhancement near the tip (compare curves 2 and 4, and curves 1 and 3 in Fig. 5a). Therefore, to achieve larger enhancement of the local field near the tip, one should increase the permittivity of the metal and decrease the permittivity of the dielectric. However, it is necessary to keep in mind that in this case, the applicability of GOA, used for the above analysis worsens (Fig. 2b), which may eventually result in increased errors of analysis and noticeable reflection of the plasmon. The determination of these errors and reflection can be done, for example, by means of numerical analysis of plasmon propagation in grooves with larger angles using the FDTD algorithm [17,18].

Increasing angle of incidence θ_0 results in a monotonous reduction of the local field enhancement at the tip of the groove (Fig. 5b). This is simply related to the fact that if the amplitude of the incident plasmon at infinity $H_{200} = 1$, and the angle of incidence θ_0 is increased, then the initial energy flux S_{0y} through the top side of the box in Fig. 4 is decreased. Due to energy conservation, this flux must be the same through the bottom side of the box (see above), but the direction of propagation of the plasmon near the tip is parallel to the y-axis, i.e. near the tip $\theta = 0$ (the same as for the case with $\theta_0 = 0$). Therefore, energy conservation suggests that at an angle of incidence $\theta_0 \neq 0$, the local field near the tip is equal to the local field at $\theta_0 = 0$ (normal incidence onto the tip – Fig. 5a) multiplied by $\sqrt{\cos(\theta_0)}$. This is in excellent agreement with curves 1, 3, and 4 in Fig. 5b.

If the angle of the groove is decreased, then the maximal enhancement is achieved at larger distances from the groove (compare curves 2 and 3 in Fig. 5b). This is because in GOA, the amplitude of the incident plasmon is a function of h that is related to the y-coordinate by means of Eq. (4). As a result, at smaller groove angles the same width of the groove is obtained at larger distances from the tip (Eq. (4)).

Though Figs. 5a,b demonstrate maximal possible enhancement of the local field during nano-focusing in a sharp metallic groove, they still do not give an idea about real achievable enhancement that is expected to strongly depend on dissipation in the metal. It is obvious that the smaller the groove angle, the larger the distance that a plasmon should propagate towards the tip in order to experience the considered field enhancement and focusing. Therefore, consideration of plasmon propagation in the presence of real dissipation in the metal is essential for proper understanding of the possibility of achieving effective nano-focusing in real metallic nano-grooves.

In the most general case of arbitrary dissipation (i.e., arbitrary complex dielectric permittivity of the metal $\varepsilon_2 = e_1 + ie_2$), instead of Eq. (14), the energy flux S in the gap plasmon in a uniform gap with constant width h is determined as

$$S = \frac{c^2}{8\pi\omega}\left|H_{20}\right|^2 \exp(-2x_p Q_2)\left[\frac{\mathrm{Re}(q/\varepsilon_2)}{\mathrm{Re}(\alpha_2)} + \frac{\mathrm{Re}(q/\varepsilon_1)}{\mathrm{Re}(\alpha_1)}\frac{\sinh[h\,\mathrm{Re}(\alpha_1)]}{2\left|\cosh(\alpha_1 h/2)\right|^2}\right.$$

$$\left. + \frac{\mathrm{Re}(q/\varepsilon_1)}{\mathrm{Im}(\alpha_1)}\frac{\sinh[h\,\mathrm{Im}(\alpha_1)]}{2\left|\cosh(\alpha_1 h/2)\right|^2}\right], \qquad (16)$$

where x_p is the coordinate in the direction of plasmon propagation, and H_{20} is the amplitude of the magnetic field at either metal interface at some arbitrary reference point along the direction of the wave propagation. Note that in the presence of dissipation, we are not able to assume that the amplitude of the incident plasmon is equal to one at $y = +\infty$, since in this case,

the amplitude of the plasmon would have been zero at any finite value of y. Therefore, instead, we assume that the amplitude of the incident plasmon $H_{20} = 1$ at some reference (finite) value of y (the specific choice of y will be explained below).

Though Eq. (16) is valid for arbitrary dissipation, below we will focus mainly on the approximation when the dissipation is weak: $Q_2 << Q_1$ (or $e_2 << |e_1|$). This is because only this situation presents an interest from the view-point of nano-focusing, noticeable propagation distances of the gap plasmons, and significant increase of their amplitudes (see below).

If the dissipation is weak ($Q_2 << Q_1$), then the imaginary part Q_2 of the wave number q can be obtained from Eq. (2):

$$Q_2 \approx \frac{\alpha_{10}^2 \varepsilon_1 e_2 (2Q_1^2 - k_0^2 e_1)}{Q_1 [h\alpha_{10}^2 \alpha_{20} e_1^2 - h\alpha_{20}^3 \varepsilon_1^2 - 2k_0^2 \varepsilon_1 e_1 (\varepsilon_1 - e_1)]}, \tag{17}$$

where Q_1 is again determined by Eq. (11) (see also Fig. 2a).

In the presence of dissipation, Eq. (13) is no longer valid, since conservation of energy in this case should also involve dissipation of the plasmon along the direction of its propagation. Therefore, the following numerical procedure has been used for the determination of plasmon amplitude as a function of distance from the tip of the groove. Consider two points on the plasmon ray (x,y) and (x + dx, y + dy), that are separated by the distance dx_0. Suppose that the angle between the ray and the y-axis at the point (x,y) is θ. Then the variation of the flux in the plasmon between the two points will consist of two parts:

$$dS = dS_0 + dS_d, \tag{18}$$

where dS_0 is the variation of the energy flux due to changing angle θ (here, the index "0" indicates that the flux variation is calculated at zero dissipation), and dS_d is the variation of the energy flux due to dissipation of the plasmon along the direction of its propagation.

As indicated above, the contribution dS_0 is calculated in the absence of dissipation. In this case, according to Eq. (13),

$$S\cos\theta = (S + dS_0)\cos(\theta + d\theta),$$

or

$$dS_0 = S\tan\theta d\theta. \tag{19}$$

The contribution dS_d is determined by differentiating Eq. (16) with respect to x_0 and assuming that H_{20} is the amplitude of the plasmon at the point (x,y). Thus,

$$dS_d = -\frac{c^2 Q_2 dx_0}{4\pi\omega}\left|H_{20}\right|^2\left[\frac{\mathrm{Re}(q/\varepsilon_2)}{\mathrm{Re}(\alpha_2)} + \frac{\mathrm{Re}(q/\varepsilon_1)}{\mathrm{Re}(\alpha_1)}\frac{\sinh[h\,\mathrm{Re}(\alpha_1)]}{2\left|\cosh(\alpha_1 h/2)\right|^2}\right.$$

$$\left. + \frac{\mathrm{Re}(q/\varepsilon_1)}{\mathrm{Im}(\alpha_1)}\frac{\sinh[h\,\mathrm{Im}(\alpha_1)]}{2\left|\cosh(\alpha_1 h/2)\right|^2}\right], \tag{20}$$

Therefore, we determine the contributions dS_0 and dS_d using Eqs. (17), (19), (20), and substitute them into Eq. (18) to determine the overall variation in the energy flux in the plasmon on its way from a point (x,y) to the point (x + dx, y + dy). This gives us the new energy flux at the point (x + dx, y + dy), and thus the amplitude of the plasmon at this point. In this way, we are able to calculate the amplitude of the plasmon at any point on the plasmon ray, if we know this amplitude at a previous close point. This immediately gives a numerical algorithm for calculating the amplitude of the plasmon as a function of y, if we know this amplitude at some reference point on the plasmon ray (i.e., at some reference distance from the tip of the groove). The value of dx is calculated from a chosen value of dy and the angle θ at the point (x,y), which is determined by Eq. (9).

The resultant numerical dependencies of the plasmon amplitude H_{20} on distance from the tip of the groove are presented in Figs. 6a,b at different wavelengths for dielectric grooves

in silver. It can be seen that the typical behavior of the presented dependencies is that as the plasmon propagates towards the tip of the groove, it amplitude decreases at large distances from the tip. It goes through a minimum, and then strongly increases reaching a maximum. Further decrease of distance to the tip of the groove results in a monotonous decrease of the plasmon amplitude (Figs. 6a,b). All the curves in Figs. 6a are normalized to the amplitude of the plasmon at the mentioned minimum. In other words, the reference point with the amplitude $H_{20} = 1$ is always chosen at the minimum of the plasmon amplitude (Figs. 6a,b).

The initial (exponential) decrease of the amplitude of the plasmon as it propagates towards the tip is related to dissipation of two uncoupled surface plasmons representing the symmetric gap plasmon at relatively large distances from the tip. In this case, the two surface plasmons hardly interact with each other (due to large h), and thus the only mechanism of changing their amplitudes is dissipation in the metal. This obviously results in an exponentially decreasing amplitude of the resultant gap plasmon with decreasing distance to the tip.

When the two surface plasmons propagate sufficiently close to the tip, where their coupling across the gap becomes noticeable, another mechanism of changing their amplitudes becomes noticeable. This is the amplitude increase due to energy conservation (see Figs. 5a,b). This mechanism overpowers dissipation and results in a substantial increase of the plasmon amplitude. As a result, the amplitude of the symmetric gap plasmon starts increasing with decreasing distance to the tip of the groove (Figs. 6a,b).

Further decrease of y results in progressively decreasing wavelength of the gap plasmon (which tends to zero as $y \rightarrow 0$ – see Fig. 2a and Eq. (6)). However, the amplitude increase due to energy conservation ceases (the curves in Figs. 5a,b reach plateaus near the tip). This means that the mechanism of decreasing amplitude due to dissipation again becomes dominant, and the curves in Figs. 6a,b, after going through maximum, start monotonously decreasing to zero near the tip of the groove.

If dissipation is strong enough, the mechanism of increasing amplitude of the gap plasmon, caused by energy conservation, may be completely suppressed. For example, this happens in the structure with $\varepsilon_2 = -16 + i$, $\varepsilon_1 = 5$, $\beta = 2^o$, $\theta_0 = 0^o$, $\lambda_{vac} = 0.6328$ μm, which does not display a maximum of plasmon amplitude, but rather its monotonous decrease to zero near the tip. Decreasing permittivity of the dielectric and increasing magnitude of the real part of the metal permittivity may result in a substantial increase of the efficiency of nano-focusing in the considered structures (Fig. 6a). This is related to the substantial increase in efficiency of the mechanism of increasing amplitude of the gap plasmon due to energy conservation in such structures (see Figs. 5a,b). Decreasing dissipation (i.e., decreasing imaginary part of the metal permittivity) obviously results in increasing maximum of the plasmon amplitude and shifting it to the left towards smaller distances from the tip (compare curves 2 and 4, and curves 1 and 3 in Fig. 6a).

Fig. 6b demonstrates the effect of the angle of incidence and the groove angle on the maximum of the plasmon amplitude during nano-focusing by sharp metallic grooves. Namely, increasing angle of the groove results in a significant increase of the amplitude maximum and shifting it to the left towards smaller distances to the tip (compare curves 1, 3 and 5 in Fig. 6b). This is expected since increasing groove angle results in more rapid variations of the width of the gap, and thus in more rapid increase of the plasmon amplitude due to the energy conservation mechanism (because the amplitude of the plasmon in this mechanism depends only on local gap width h – see Figs. 5a,b and Eq. (4)). This means that the effect of dissipation will be diminished, because the amplitude of the plasmon is increased by the energy conservation mechanism within smaller distance intervals. Thus the mechanism of increasing plasmon amplitude becomes more dominant. As a result, the amplitude maximum is reached at smaller distances to the tip, and it is higher than for smaller groove angles.

Increasing angle of incidence θ_0 results in decreasing maximum amplitude (compare curves 1 and 2, and 3 and 4 in Fig. 6b). This effect has the same explanation as in the case

without dissipation and is related to decreasing the y-component of the energy flux in the incident plasmon at the reference point (see above).

Note that the suggested choice of the reference points for the incident plasmons (with $H_{20} = 1$) at the distance from the tip where the plasmon amplitude reaches the minimum is convenient, since it immediately gives the information about the maximal possible enhancement of the local field in the considered structure with dissipation. This enhancement is thus given by the value of the plasmon amplitude at the point of its maximal increase (Figs. 6a,b). For example, up to ~ 5 times enhancement of the local field can easily be achieved in the considered structures. Such a situation can be achieved in practice by using the end-fire excitation of the incident plasmon in a groove (gap) of ~ 10 μm deep (this depth corresponds to the minimum amplitude in Figs. 6a,b). Use of deeper grooves will result in additional energy losses in the focused plasmon on its way towards the point with the minimal amplitude. Use of shallower grooves will result in less efficient enhancement, which in this case will be given by the ratio of the maximal amplitude (Figs. 6a,b) to the amplitude at the point of the end-fire excitation, which will be somewhere between the maximum and minimum of the plasmon amplitude in Figs. 6a,b. Thus the position of the minimum on the dependencies of the plasmon amplitude on distance from the tip of the groove (Figs. 6a,b) determines the optimal depth of the groove for maximal plasmon focusing and local field enhancement.

Numerical verification of the proposed geometrical optics approach can be conducted using FDTD algorithm [41]. In particular, it has been shown that for the considered structures with $\beta = 5^o$ and normal incidence of the gap plasmon ($\theta_0 = 0$), the difference between the approximate theory based on the geometrical optics approach and the numerical analysis is ~ 5% [41]. Since this groove angle corresponds to the boarder line for the applicability of GOA, the obtained agreement can be regarded as very good. Note however, that due to its numerical inefficiency, the FDTD approach can hardly be used for the analysis of nano-focusing in grooves with smaller angles and at non-normal incidence ($\theta_0 \neq 0$) [41]. This is because of

very strong localization of the gap plasmons during nano-focusing and large propagation distances (~ 10 μm – see above), which requires very fine discretization of the structure in three dimensions within large distances. On the other hand, GOA is not applicable for grooves with $\beta \geq \beta_{c2} \sim 7^{o}$. This makes the numerical FDTD analysis [41] and the presented GOA approach rather complimentary to each other.

5. CHANNEL PLASMON-POLARITONS

In the previous sections, we considered propagation of gap plasmons incident onto the tip of a sufficiently sharp dielectric groove in a metal by means of GOA. On the other hand, it has been demonstrated in our previous publications [17,18] that V-shaped grooves can support a new type of plasmonic modes that are strongly localized near the tip of the groove and propagate along it. In particular, it has been shown that CPPs can exist only if the groove angle β is smaller than a critical angle β_{c1} (which in the case of the silver-vacuum structure and $\lambda_{vac} = 0.6328$ μm is $\beta_{c1} \approx 75^{o}$ [17]).

The analysis of the CPP modes in V-grooves has been conducted by means of the FDTD algorithm [17,18]. However, it is possible to expect that GOA might also be used for the analysis of CPP modes in sufficiently sharp grooves. The effective permittivity for the symmetric gap plasmon propagating in such a groove is defined as $\varepsilon_{eff} = [Q_1(y)c/\omega]^{1/2}$. It increases with decreasing distance to the tip of the groove, due to increasing Q_1 (see Eq. (6) and Fig. 2a). Thus the groove forms a kind of a waveguide for gap plasmons with gradually changing permittivity ε_{eff}. A CPP mode could then be represented by a symmetric gap plasmon successively reflecting from the tip of the groove and the turning point (simple caustic) – Fig. 7. The wave vector for the CPP mode is equal to the x-component of the wave vector of the symmetric gap plasmon $q_{cpp} = Q_{1x}$.

Note that the main difference between this situation and the previously considered nano-focusing of symmetric gap plasmons is that in the case of a CPP mode no incident gap plasmon should exist. The gap plasmon representing the CPP mode should be confined to a region close to the tip of the groove and cannot leave this region, because CPP modes are non-radiative structural eigenmodes [17,18,20]. This is very similar to a non-radiative mode guided by a dielectric slab.

Note that this method of analysis of CPP modes is analogous to the geometrical acoustic approach used for the investigation of localized acoustic modes propagating along a sufficiently sharp elastic wedge [41,42].

Only symmetric gap plasmons can be used for the representation of CPP modes. This is because the effective permittivity for an antisymmetric gap plasmon (as well as its wave vector) decreases with decreasing distance from the tip of the groove. As a result, no guiding effect near the tip of the groove can be achieved in this case.

The turning point y_t (simple caustic) is then determined by the condition $Q_1(y)\big|_{y=y_t} = q_{cpp}$. In this case, the gap plasmon representing the CPP mode propagates parallel to the tip of the groove (Fig. 7).

All this is very similar to acoustic waves in acute elastic wedges [41,42]. However, the major difference is that if $h \to 0$, then $Q_1 \propto h^{-1}$ (see Eq. (6)), whereas in acoustics the corresponding wave vector of the plate mode was $\propto h^{-1/2}$ [41,42]. As a result, the Bohr-Sommerfeld quantization condition [41,42]

$$\int_0^{y_t} \sqrt{Q_1^2 - q_{cpp}^2}\, dy = \pi n \qquad (n = 1, 2, 3, \ldots), \tag{21}$$

that should be used for determination of wave vectors of CPPs results in a diverging (at zero) integral. Therefore, it cannot be used for the determination of dispersion of CPP modes.

Physically, this is related to the fact that if GOA is applicable near the tip of the groove (see conditions (1), (7) and (8)), then a symmetric gap plasmon propagating towards the tip at any possible angle θ will travel an infinite optical path until it reaches the tip. As indicated above, such plasmons cannot be reflected back from the tip even if dissipation is disregarded. The plasmon asymptotically stops at the tip and will have infinite localization. As a result, the localization of the corresponding CPP mode near the tip of the groove will also be infinite, $q_{cpp} = +\infty$, and this corresponds to zero wavelength and velocity. In other words, the CPP mode does not exist in the considered structure.

Thus CPP modes do not exist in a groove if GOA is applicable. On the contrary, if GOA is not applicable near the tip of the V-groove, then the integral in Eq. (21) and its divergence at y = 0 do not have a physical meaning. The gap plasmon representing a CPP mode does not propagate up to the tip of the groove, but rather is reflected on its way there. Thus, the CPP mode can indeed be represented by a gap mode successively reflecting from the tip of the groove and the turning point. However, GOA cannot be used in this case for the determination of dispersion of CPP modes, and other methods have to be used instead [17,18,20].

Nevertheless, the above consideration of CPP modes in GOA have lead to one important result. This is the conclusion that CPP modes can exist only if GOA is not applicable near the tip of the groove. Thus, according to the applicability condition of GOA near the tip (Eqs. (7) and (8)), we can write the existence condition for CPP modes in a V-groove as follows:

$$\beta \gtrsim \beta_{c2}. \tag{22}$$

This condition is thus opposite to inequality (8). It determines a lower critical angle β_{c2} below which CPP modes do not exist in a V-shaped groove. Thus, CPPs exist only within the range of angles:

$$\beta_{c2} \lesssim \beta < \beta_{c1}, \tag{23}$$

where β_{c1} was determined numerically in [17] as the upper critical angle above which CPPs do not exist because they become coupled to surface plasmons on the sides of the groove [17]. Now it is clear why we used the index "2" for the critical angle β_{c2} (see also Eq. (8)). This is because of the existence of two critical angles determining the existence condition for CPP modes in metallic V-grooves. For example, for a silver-vacuum V-groove at the vacuum wavelength $\lambda_{vac} = 0.6328$ μm, we have $\beta_{c1} \approx 75^o$ [17], and $\beta_{c2} \approx 7^o$ (see above).

Note that the existence of the lower critical angle is difficult to demonstrate using the FDTD algorithm. This is because it is hardly possible to conduct FDTD analysis of CPPs with infinite (or very large) localization that is typical near or below the lower critical angle (see also the end of Section 4).

6. CONCLUSIONS

A possibility of effective nano-focusing of symmetric gap plasmons in metallic V-grooves with sufficiently small angles has been demonstrated by means of the geometrical optics approximation. It has been shown in the approximation of continuous electrodynamics that such two-dimensional plasmons asymptotically stop at the tip of the groove with both their phase and group velocities tending to zero, and the wave vector to infinity. As a result, any symmetric gap plasmon incident onto the tip of the groove at any initial angle will not experience reflection from the tip. It will rather propagate an infinite optical path until it reaches the tip, and thus eventually dissipates in the metal.

As the plasmon propagates towards the tip of the groove, its amplitude has been shown to increase substantially, but to a finite value (contrary to the focusing in a tapered metallic tip [27]). The effect of dissipation on the nano-focusing by means of a metallic V-groove was analyzed in detail. In particular, a method for optimizing the groove for achieving maximal local field enhancement was described. The effect of angle of incidence and structural parameters of the groove on nano-focusing and local field enhancement was investigated

theoretically. Applicability conditions for the obtained results and the used geometrical optics approach were derived and discussed.

The analysis of channel plasmon-polaritons in V-grooves by means of GOA demonstrated the impossibility of using this method for the determination of dispersion of CPPs in sharp V-shaped grooves, due to divergence of the integral in the Bohr-Sommerfeld condition. However, it has also been shown that a CPP mode can nevertheless be represented by a symmetric gap plasmon successively reflecting from the tip of the groove and the turning point. Thus this plasmon is guided by the groove, forming a CPP mode. In addition, this consideration has resulted in the derivation of a new existence condition for CPP modes in V-shaped grooves. This condition introduced the second (lower) critical angle of the groove, below which CPP modes do not exist, since they appear to be infinitely localized near the tip and thus have zero velocity. Only if the groove angle exceeds the lower critical angle can CPP modes exist in a V-groove. Combined with the upper critical angle (above which CPP do not exist [17]), the determined lower critical angle gives the range of groove angles for which CPPs can propagate along a V-groove and have sub-wavelength localization [17,18].

The conducted analysis of existence conditions for CPPs in V-grooves is particularly important since the developed numerical methods of analysis largely fail at the considered small groove angles [17]. The obtained results will also be important for further development of near-field optical microscopy [22-29] and deeper understanding of physical phenomena resulting from interaction of electromagnetic waves with metallic nano-structures.

References

1. W. L. Barnes, A. Dereux, T. W. Ebbesen, Nature, **424**, 824 (2003).
2. A. V. Zayats and I. Smolyaninov, J. Opt. A: Pure Appl. Opt., **5**, S16 (2003).
3. J. R. Krenn, Nature Mater. **2**, 210 (2003).
4. S. A. Maier, P. G. Kik, H. A. Atwater, S. Meltzer, E.Harel, B. E. Koel, and A. A. G. Requicha, Nature Mater. **2**, 229 (2003).
5. M. Quinten, A. Leitner, J. R. Krenn, and F. R. Aussenegg, Opt. Lett. **23**, 1331 (1998).
6. J. Takahara, S. Yamagishi, H. Taki, A. Morimoto, and T. Kobayashi, Opt. Lett. **22**, 475 (1997).
7. T. Onuki, Y. Watanabe, K. Nishio, T. Tsuchiya, T. Tani, and T. Tokizaki, J. Microscopy **210**, 284 (2003).
8. P. Berini, Phys. Rev. **B61**, 10484 (2000); Phys Rev. **B63**, 125417 (2001).
9. G. Schider, J. R. Krenn, A. Hohenau, H. Ditlbacher, A. Leitner, F. R. Aussenegg, W. L. Schaich, I. Puscasu, B. Monacelli, and G. Boreman, Phys. Rev. **B68**, 155427 (2003).
10. J. R. Krenn, B. Lamprecht, H. Ditlbacher, G. Schider, M. Salerno, A. Leitner, and F. R. Aussenegg, Europhys. Lett., **60**, 663 (2002).
11. J.-C. Weeber, A. Dereux, C. Girard, J. R. Krenn, and J.-P. Goudonnet, Phys. Rev. B **60**, 9061, (1999-II).
12. T. Yatsui, M. Kougori, and M. Ohtsu, Appl. Phys. Lett. **79**, 4583 (2001).
13. M. Ohtsu, K. Kobayashi, T. Kawazoe, S. Sangu, and T. Yatsui, IEEE J. of Selected Topics in Quantum Electron. **8**, 839 (2002).
14. K. Tanaka and M. Tanaka, Appl. Phys. Lett. **82**, 1158 (2003).
15. K. Tanaka, M. Tanaka, and T. Sugiyama, Optics Express, **13**, 256 (2005).
16. B. Wang and G. P. Wang, Appl. Phys Lett., **85**, 3599 (2004).
17. D. F. P. Pile and D. K. Gramotnev, Opt. Lett. **29**, 1069 (2004).
18. D. K. Gramotnev and D. F. P. Pile, Appl. Phys. Lett. **85**, 6323 (2004).

19. D. F. P. Pile and D. K. Gramotnev, Opt. Lett. **30**, 1186 (2005).

20. I. V. Novikov and A. A. Maradudin, Phys. Rev. **B66**, 035403 (2002).

21. D. F. P. Pile and D. K. Gramotnev, Appl. Phys. Lett. **86**, 161101 (2005).

22. D. W. Pohl, W. Denk, and M. Lanz, Appl. Phys. Lett. **44**, 651 (1984).

23. L. Novotny and C. Hafner, Phys Rev. E **50**, 4094 (1994).

24. A. Bouhelier, J. Renger, M. R. Beversluis, L. Novotny, J. Microsc., **210**, 220 (2003).

25. F. Keilmann, J. Microsc., **194**, 567 (1999).

26. H. G. Frey, F. Keilmann, A. Kriele, and R. Guckenberger, Appl Phys. Lett. **81**, 5030 (2002).

27. M. I. Stockman, Phys. Rev. Lett., **93**, 137404, (2004).

28. Topics in Applied Physics: Near-field Optics and surface plasmon-polaritons, vol. 81, ed: S. Kawata (Springer-Verlag, Berlin, 2001).

29. A. Naber, D. Molenda, U. C. Fischer, H.-J. Maas, C. Hoppener, N. Lu, and H. Fuchs, Phys Rev Lett., **89**, 210801, (2002).

30. A. Hartschuh, H. N. Pedrosa, L. Novotny, and T. D. Krauss, Science, **301**, 1354 (2003).

31. K. Kneipp, Y. Wang, H. Kneipp, L. T. Perelman, I. Itzkan, R. R. Dasari, and M. S. Feld, Phys. Rev. Lett., **78**, 1667 (1997).

32. S. M. Nie and S. R. Emery, Science **275**, 1102 (1997).

33. B. Pettinger, B. Ren, G. Picardi, R. Schuster, G. Ertl, *Phys. Rev. Lett.*, **92**, 096101 (2004).

34. T. Ichimura, N. Hayazawa, M. Hashimoto, Y. Inouye, S. Kawata, *Phys. Rev. Lett.*, **92**, 220801 (2004).

35. H. Raether, *Surface Plasmons* (Springer-Verlag, Berlin, 1988)

36. Yu. A. Kravtsov, Yu. I. Orlov, *Geomentrical Optics of Inhomogeneous Media* (Springer-Verlag, Berlin, 1990).

37. E. D. Palik, *Handbook of Optical Constants of Solids* (Academic, New York, 1985).

38. Christensen, D. Fowers, Biosens. Bioelectron. **11**, 677 (1996); D. Fowers, *Masters Thesis*, University of Utah (1994).

39. A. Liebsch, Phys. Rev. Lett., **54**, 67 (1985).

40. I. A. Larkin, M. I. Stockman, M. Achermann, and V. I. Klimov, Phys. Rev B **69**, 121403(R) (2004).

41. D. F. P. Pile and D. K. Gramotnev, Non-adiabatic nano-focusing in metallic V-shaped grooves, (to be published).

42. V. V. Krylov, Sov. Phys. Tech. Phys. **35(2)**, 137 (1990).

43. V. V. Krylov, Sov. Phys. Acoust. **36(2)**, 176 (1989).

FIGURE CAPTIONS

Fig. 1. (a) The analyzed structure with a dielectric groove of angle β. ε_1 is the permittivity of the dielectric filling the groove, and ε_2 is the metal permittivity. (b) A ray representing the direction of propagation of a symmetric gap plasmon in the groove in the geometrical optics approximation. θ_0 is the angle of propagation of the gap plasmon at large distances from the tip of the groove, where the coupling between the two surface plasmons representing the gap plasmon is negligible.

Fig. 2. a) The dependencies of the wave number Q_1 of the symmetric gap plasmon on gap width h for the following parameters: (1) $e_1 = -6.5$, $\varepsilon_1 = 1$, vacuum wavelength $\lambda_{vac} = 0.4592$ μm, (2) $e_1 = -16$, $\varepsilon_1 = 1$, $\lambda_{vac} = 0.6328$ μm, (3) $e_1 = -58.8$, $\varepsilon_1 = 2.5$, $\lambda_{vac} = 1.127$ μm, (4) $e_1 = -58.8$, $\varepsilon_1 = 1$, $\lambda_{vac} = 1.127$ μm. b) The dependencies of the left-hand side of inequality (1) on distance from the tip of the groove with the angle $\beta = 2^o$ for the following parameters: (1) $e_1 = -96.6$, $\varepsilon_1 = 2.5$, $\lambda_{vac} = 1.631$ μm, (2) $e_1 = -58.8$, $\varepsilon_1 = 2.5$, $\lambda_{vac} = 1.127$ μm, (3) $e_1 = -16$, $\varepsilon_1 = 1$, $\lambda_{vac} = 0.6328$ μm, (4) $e_1 = -58.8$, $\varepsilon_1 = 5$, $\lambda_{vac} = 1.127$ μm, (5) $e_1 = -16$, $\varepsilon_1 = 2.5$, $\lambda_{vac} = 0.6328$ μm. Curve 3 in (b) also approximately corresponds to the other structure with $e_1 = -58.8$, $\varepsilon_1 = 2.5$, $\lambda_{vac} = 1.127$ μm, and $\beta = 1^o$. The metal permittivities correspond to silver at the indicated wavelengths [37,38].

Fig. 3. Typical plasmon rays in the silver-vacuum grooves with the angles: 1) $\beta = 1^o$, 2) $\beta = 2^o$, and 3) $\beta = 5^o$. Three different angles of incidence are considered: Dashed curves: $\theta_0 = 75^o$, Solid curves: $\theta_0 = 45^o$, and Dotted curves: $\theta_0 = 25^o$. The initial y-coordinates for all the rays correspond to the same width of the groove (gap): $h \approx 28.3$ nm. The permittivities are for the silver-vacuum structure at $\lambda_{vac} = 0.6328$ μm: $\varepsilon_1 = 1$, $e_1 = -16$ [37,38].

Fig. 4. Imaginary box containing the groove for the determination of energy conservation in the incident gap plasmon. The box extends into the positive and negative z-directions into the regions where the plasmon field is negligible (or it is infinitely long along the z-axis).

Fig. 5. a) The dependencies of the normalized amplitude of the magnetic field in the metal $H_{20}(y)/H_{200}$ ($H_{200} \equiv H_{20}(\infty)$) in a symmetric gap plasmon incident onto the tip of the groove on distance to the tip in the absence of dissipation at the angle of incidence $\theta_0 = 0$, the groove angle $\beta = 2^o$, and different permittivities of the metal and dielectric in the groove: (1) $e_1 = -58.8$, $\varepsilon_1 = 2.5$, $\lambda_{vac} = 1.127$ μm, (2) $e_1 = -16$, $\varepsilon_1 = 1$, $\lambda_{vac} = 0.6328$ μm, (3) $e_1 = -58.8$, $\varepsilon_1 = 5$, $\lambda_{vac} = 1.127$ μm, (4) $e_1 = -16$, $\varepsilon_1 = 2.5$, $\lambda_{vac} = 0.6328$ μm. b) The dependencies $H_{20}(y)/H_{200}$ for a symmetric plasmon at $e_1 = -16$, $\varepsilon_1 = 1$, $\lambda_{vac} = 0.6328$ μm, and different values of θ_0 and β: (1), $\theta_0 = 0$, $\beta = 4^o$, (2) $\theta_0 = 45^o$, $\beta = 1^o$, (3) $\theta_0 = 45^o$, $\beta = 4^o$, (4) $\theta_0 = 75^o$, $\beta = 4^o$. The metal permittivities correspond to silver at the indicated wavelengths [37,38].

Fig. 6. The y-dependencies of the normalized amplitude of the magnetic field in the metal $H_{20}(y)/H_{20min}$ (H_{20min} is the amplitude of the plasmon at the local minimum of the amplitude) in a symmetric gap plasmon incident onto the tip of the groove in the presence of dissipation. a) Same values of $\theta_0 = 0$, $\beta = 2^o$, but different permittivities: 1) $\varepsilon_2 = -58.8 + i$ (does not correspond to a particular metal), $\varepsilon_1 = 2.5$, $\lambda_{vac} = 1.127$ μm; 2) $\varepsilon_2 = -16 + 0.52i$ (Ag [38]), $\varepsilon_1 = 1$, $\lambda_{vac} = 0.6328$ μm; (3) $\varepsilon_2 = -58.8 + 3.85i$ (Ag [37]), $\varepsilon_1 = 2.5$, $\lambda_{vac} = 1.127$ μm; (4) $\varepsilon_2 = -16 + i$ (Ag [37]), $\varepsilon_1 = 1$, $\lambda_{vac} = 0.6328$ μm; (5) $\varepsilon_2 = -16 + i$ (Ag [37]), $\varepsilon_1 = 2.5$, $\lambda_{vac} = 0.6328$ μm. b) Permittivities $\varepsilon_2 = -16 + 0.52i$, $\varepsilon_1 = 1$, $\lambda_{vac} = 0.6328$ μm, but different angles: (1) $\theta_0 = 0$, $\beta = 4^o$, (2) $\theta_0 = 45^o$, $\beta = 4^o$, (3) $\theta_0 = 0$, $\beta = 2^o$, (4) $\theta_0 = 45^o$, $\beta = 2^o$, (5) $\theta_0 = 0$, $\beta = 1^o$.

Fig. 7. Geometrical optics representation of a CPP mode in a metallic V-groove with the tip at y = 0. The symmetric gap plasmon with the wave vector $\mathbf{Q}_1(y)$, representing the CPP

mode, is successively reflected from the tip of the groove and the turning point (caustic); the wave vector of the CPP mode $q_{cpp} = Q_{1x}$.

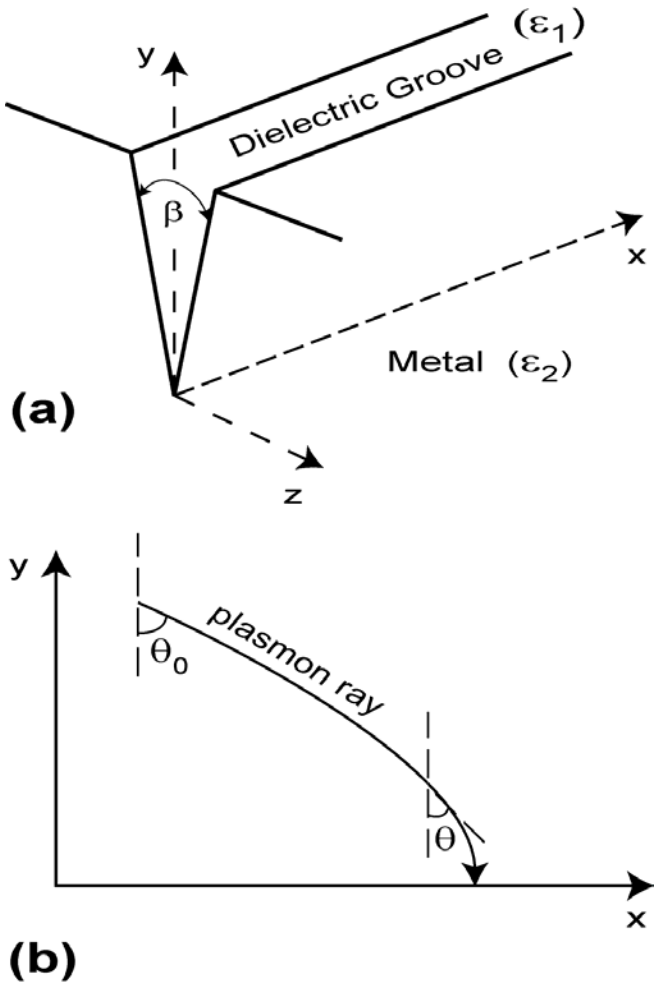

Fig. 1. (a) The analyzed structure with a dielectric groove of angle β. ε_1 is the permittivity of the dielectric filling the groove, and ε_2 is the metal permittivity. (b) A ray representing the direction of propagation of a symmetric gap plasmon in the groove in the geometrical optics approximation. θ_0 is the angle of propagation of the gap plasmon at large distances from the tip of the groove, where the coupling between the two surface plasmons representing the gap plasmon is negligible.

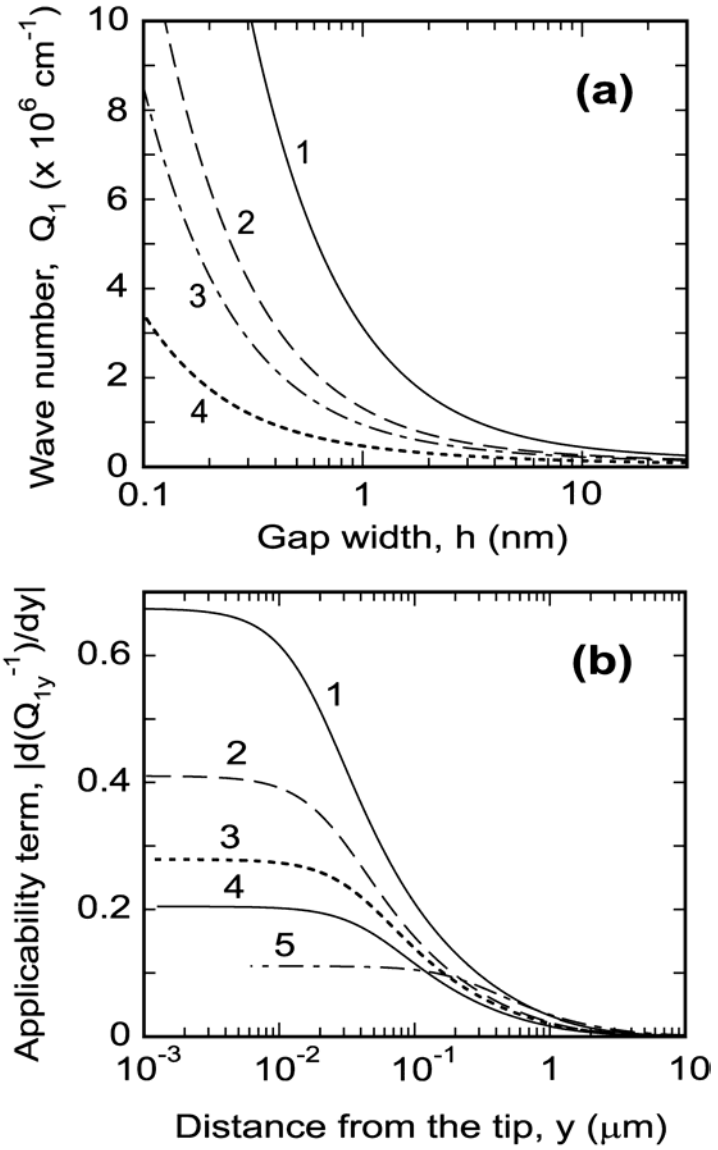

Fig. 2. a) The dependencies of the wave number Q_1 of the symmetric gap plasmon on gap width h for the following parameters: (1) $e_1 = -6.5$, $\varepsilon_1 = 1$, vacuum wavelength $\lambda_{vac} = 0.4592$ μm, (2) $e_1 = -16$, $\varepsilon_1 = 1$, $\lambda_{vac} = 0.6328$ μm, (3) $e_1 = -58.8$, $\varepsilon_1 = 2.5$, $\lambda_{vac} = 1.127$ μm, (4) $e_1 = -58.8$, $\varepsilon_1 = 1$, $\lambda_{vac} = 1.127$ μm. b) The dependencies of the left-hand side of inequality (1) on distance from the tip of the groove with the angle $\beta = 2^o$ for the following parameters: (1) $e_1 = -96.6$, $\varepsilon_1 = 2.5$, $\lambda_{vac} = 1.631$ μm, (2) $e_1 = -58.8$, $\varepsilon_1 = 2.5$, $\lambda_{vac} = 1.127$ μm, (3) $e_1 = -16$, $\varepsilon_1 = 1$, $\lambda_{vac} = 0.6328$ μm, (4) $e_1 = -58.8$, $\varepsilon_1 = 5$, $\lambda_{vac} = 1.127$ μm, (5) $e_1 = -16$, $\varepsilon_1 = 2.5$, $\lambda_{vac} = 0.6328$ μm. Curve 3 in (b) also approximately corresponds to the other structure with $e_1 = -58.8$, $\varepsilon_1 = 2.5$, $\lambda_{vac} = 1.127$ μm, and $\beta = 1^o$. The metal permittivities correspond to silver at the indicated wavelengths [37,38].

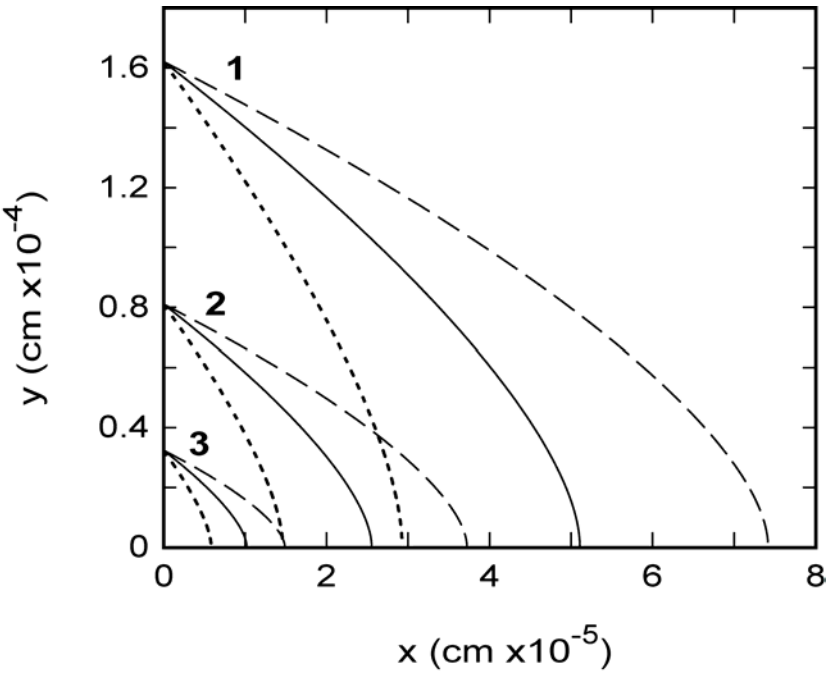

Fig. 3. Typical plasmon rays in the silver-vacuum grooves with the angles: 1) $\beta = 1^o$, 2) $\beta = 2^o$, and 3) $\beta = 5^o$. Three different angles of incidence are considered: Dashed curves: $\theta_0 = 75^o$, Solid curves: $\theta_0 = 45^o$, and Dotted curves: $\theta_0 = 25^o$. The initial y-coordinates for all the rays correspond to the same width of the groove (gap): $h \approx 28.3$ nm. The permittivities are for the silver-vacuum structure at $\lambda_{vac} = 0.6328$ μm: $\varepsilon_1 = 1$, $e_1 = -16$ [37,38].

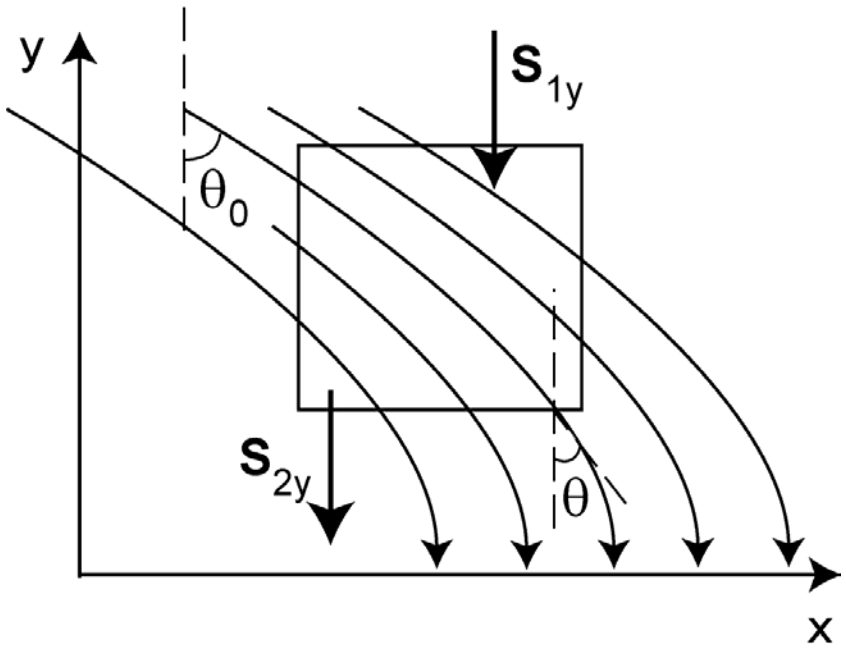

Fig. 4. Imaginary box containing the groove for the determination of energy conservation in the incident gap plasmon. The box extends into the positive and negative z-directions into the regions where the plasmon field is negligible (or it is infinitely long along the z-axis).

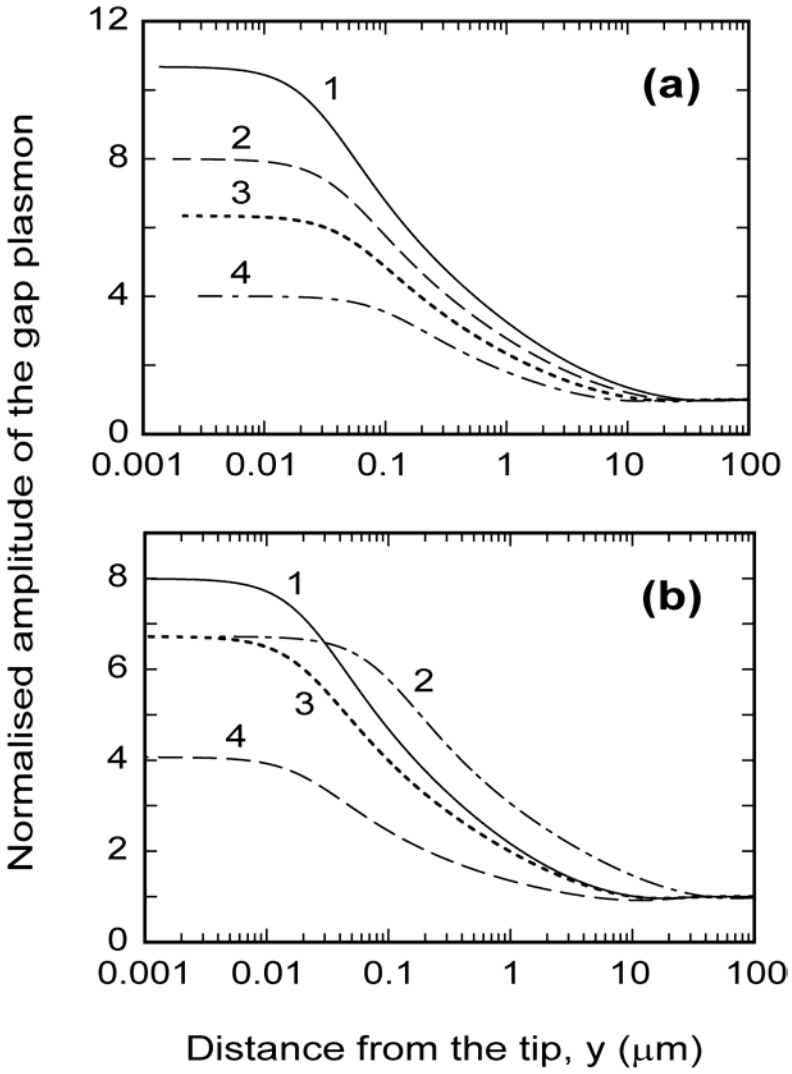

Fig. 5. a) The dependencies of the normalized amplitude of the magnetic field in the metal $H_{20}(y)/H_{200}$ ($H_{200} \equiv H_{20}(\infty)$) in a symmetric gap plasmon incident onto the tip of the groove on distance to the tip in the absence of dissipation at the angle of incidence $\theta_0 = 0$, the groove angle $\beta = 2^o$, and different permittivities of the metal and dielectric in the groove: (1) $e_1 = -58.8$, $\varepsilon_1 = 2.5$, $\lambda_{vac} = 1.127$ μm, (2) $e_1 = -16$, $\varepsilon_1 = 1$, $\lambda_{vac} = 0.6328$ μm, (3) $e_1 = -58.8$, $\varepsilon_1 = 5$, $\lambda_{vac} = 1.127$ μm, (4) $e_1 = -16$, $\varepsilon_1 = 2.5$, $\lambda_{vac} = 0.6328$ μm. b) The dependencies $H_{20}(y)/H_{200}$ for a symmetric plasmon at $e_1 = -16$, $\varepsilon_1 = 1$, $\lambda_{vac} = 0.6328$ μm, and different values of θ_0 and β: (1), $\theta_0 = 0$, $\beta = 4^o$, (2) $\theta_0 = 45^o$, $\beta = 1^o$, (3) $\theta_0 = 45^o$, $\beta = 4^o$, (4) $\theta_0 = 75^o$, $\beta = 4^o$. The metal permittivities correspond to silver at the indicated wavelengths [37,38].

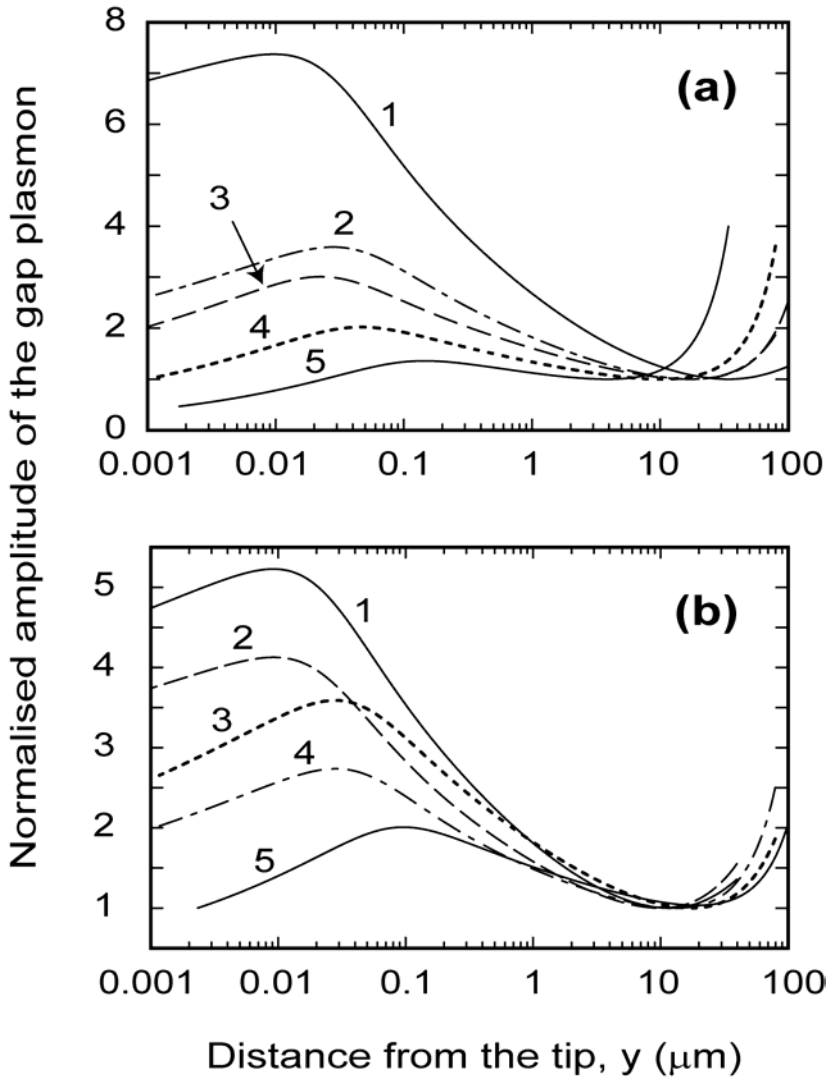

Fig. 6. The y-dependencies of the normalized amplitude of the magnetic field in the metal $H_{20}(y)/H_{20min}$ (H_{20min} is the amplitude of the plasmon at the local minimum of the amplitude) in a symmetric gap plasmon incident onto the tip of the groove in the presence of dissipation. a) Same values of $\theta_0 = 0$, $\beta = 2^o$, but different permittivities: 1) $\varepsilon_2 = -58.8 + i$ (does not correspond to a particular metal), $\varepsilon_1 = 2.5$, $\lambda_{vac} = 1.127$ μm; 2) $\varepsilon_2 = -16 + 0.52i$ (Ag [38]), $\varepsilon_1 = 1$, $\lambda_{vac} = 0.6328$ μm; (3) $\varepsilon_2 = -58.8 + 3.85i$ (Ag [37]), $\varepsilon_1 = 2.5$, $\lambda_{vac} = 1.127$ μm; (4) $\varepsilon_2 = -16 + i$ (Ag [37]), $\varepsilon_1 = 1$, $\lambda_{vac} = 0.6328$ μm; (5) $\varepsilon_2 = -16 + i$ (Ag [37]), $\varepsilon_1 = 2.5$, $\lambda_{vac} = 0.6328$ μm. b) Permittivities $\varepsilon_2 = -16 + 0.52i$, $\varepsilon_1 = 1$, $\lambda_{vac} = 0.6328$ μm, but different angles: (1) $\theta_0 = 0$, $\beta = 4^o$, (2) $\theta_0 = 45^o$, $\beta = 4^o$, (3) $\theta_0 = 0$, $\beta = 2^o$, (4) $\theta_0 = 45^o$, $\beta = 2^o$, (5) $\theta_0 = 0$, $\beta = 1^o$.

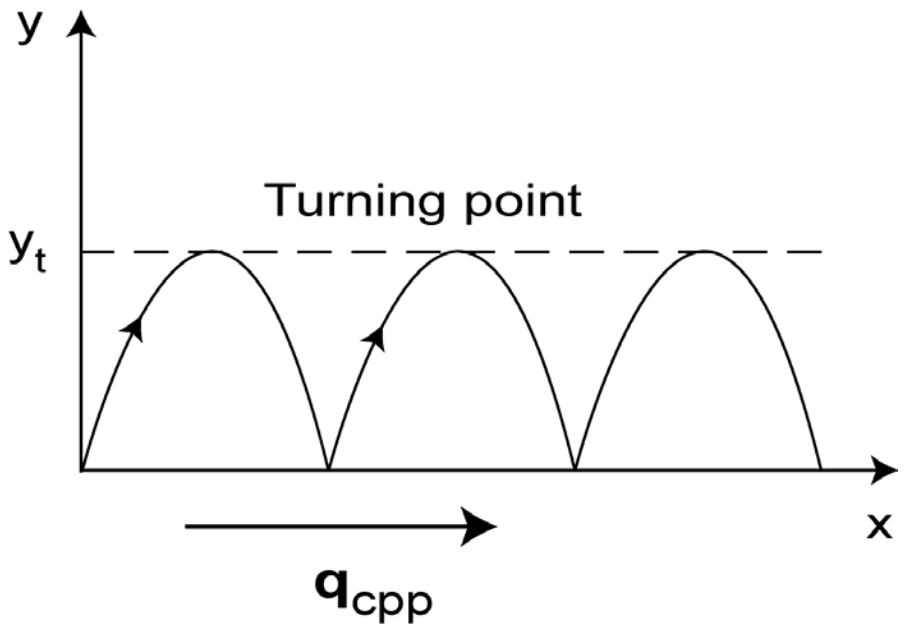

Fig. 7. Geometrical optics representation of a CPP mode in a metallic V-groove with the tip at y = 0. The symmetric gap plasmon with the wave vector $\mathbf{Q}_1(y)$, representing the CPP mode, is successively reflected from the tip of the groove and the turning point (caustic); the wave vector of the CPP mode $q_{cpp} = Q_{1x}$.